nature immunology

SUPPLEMENTARY INFORMATION

https://doi.org/10.1038/s41590-018-0230-z

In the format provided by the authors and unedited.

Human retinoic acid–regulated CD161^{+} regulatory T cells support wound repair in intestinal mucosa

Giovanni A. M. Povoleri[1,2], Estefania Nova-Lamperti[1,2], Cristiano Scottà[1,2], Giorgia Fanelli[1,2], Yun-Ching Chen[3], Pablo D. Becker[1,2], Dominic Boardman[1,2], Benedetta Costantini[4], Marco Romano[1,2], Polychronis Pavlidis[1,2], Reuben McGregor[1,2], Eirini Pantazi[1,2], Daniel Chauss[5], Hong-Wei Sun[6], Han-Yu Shih[7], David J. Cousins[8], Nichola Cooper[9], Nick Powell[1,2], Claudia Kemper[10], Mehdi Pirooznia[3], Arian Laurence[11], Shahram Kordasti[4], Majid Kazemian[12], Giovanna Lombardi[1,2,14] and Behdad Afzali[1,5,13,14]*

[1]MRC, Centre for Transplantation, King's College London, London, UK. [2]National Institute for Health Research Biomedical Research Centre at Guy's and St Thomas' NHS Foundation Trust and King's College London, London, UK. [3]Bioinformatics and Computational Biology Core, National Heart, Lung, and Blood Institute, National Institutes of Health, Bethesda, MD, USA. [4]Comprehensive Cancer Centre, School of Cancer and Pharmaceutical Sciences, King's College London, London, UK. [5]Immunoregulation Section, Kidney Diseases Branch, National Institute of Diabetes and Digestive and Kidney Diseases, National Institutes of Health, Bethesda, MD, USA. [6]Biodata Mining and Discovery Section, National Institute of Arthritis and Musculoskeletal and Skin Diseases, National Institutes of Health, Bethesda, MD, USA. [7]Lymphocyte Cell Biology Section, Molecular Immunology and Inflammation Branch, National Institute of Arthritis and Musculoskeletal and Skin Diseases, National Institutes of Health, Bethesda, MD, USA. [8]Department of Infection, Immunity and Inflammation, NIHR Leicester Respiratory Biomedical Research Unit, University of Leicester, Leicester, UK. [9]Department of Medicine, Imperial College London, London, UK. [10]Complement and Inflammation Research Section, National Heart Lung and Blood Institute, National Institutes of Health, Bethesda, MD, USA. [11]Institute of Cellular Medicine, Newcastle University, Newcastle, UK. [12]Departments of Biochemistry and Computer Science, Purdue University, West Lafayette, IN, USA. [13]National Heart, Lung, and Blood Institute, National Institutes of Health, Bethesda, MD, USA. [14]These authors contributed equally: Giovanna Lombardi, Behdad Afzali. *e-mail: behdad.afzali@nih.gov

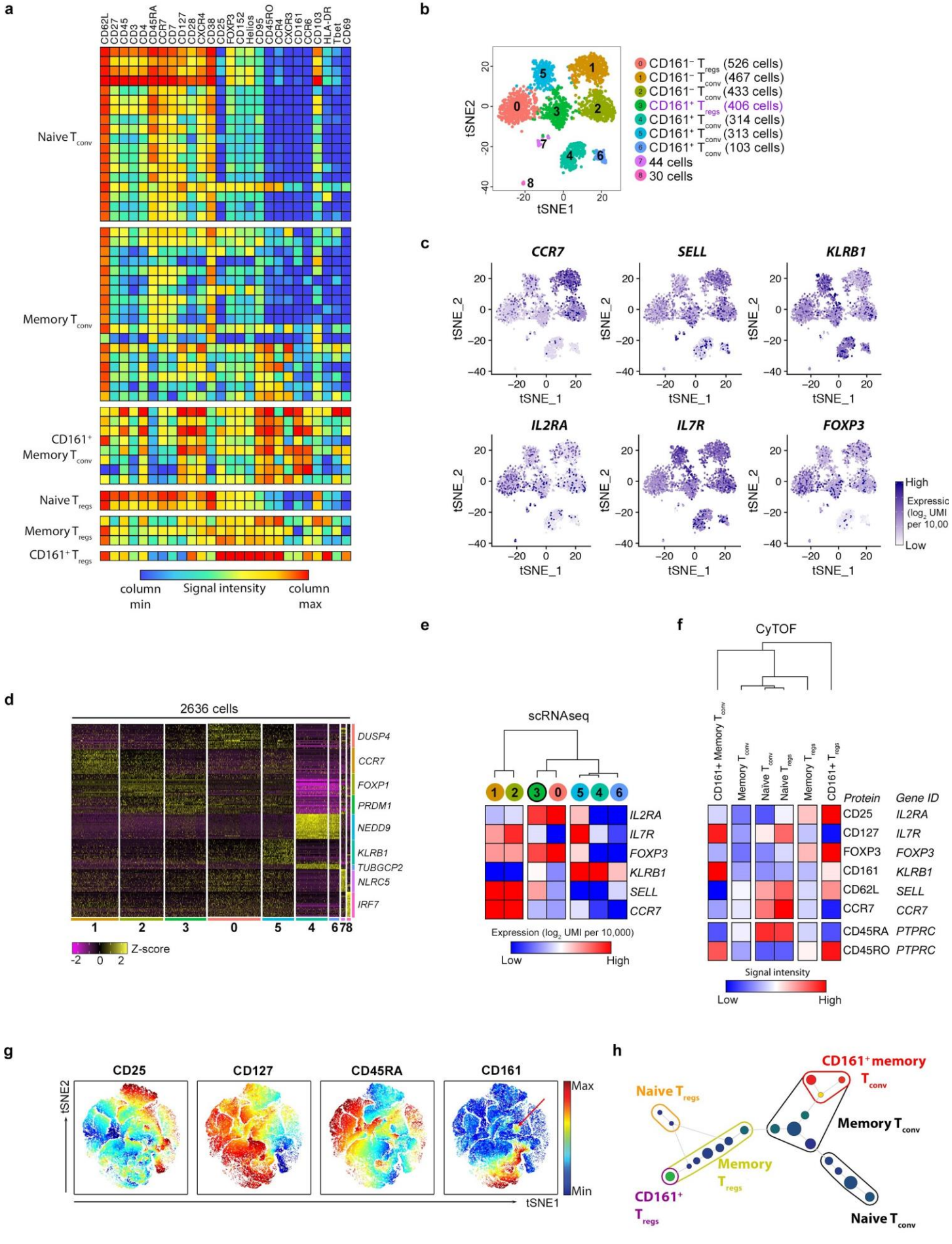
a
CD62L
CD27
CD45
CD3
CD4
CD45RA
CCR7
CD7
CD127
CD28
CXCR4
CD38
CD25
FOXP3
CD152
Helios
CD95
CD45RO
CCR4
CXCR3
CD161
CCR6
CD103
HLA-DR
Tbet
CD69
Naive T conv
Memory T conv
CD161+ Memory T conv
Naive T regs
Memory T regs
CD161+ T regs
column min
Signal intensity
column max
b
0 CD161− T regs (526 cells)
1 CD161− T conv (467 cells)
2 CD161− T conv (433 cells)
3 CD161+ T regs (406 cells)
4 CD161+ T conv (314 cells)
5 CD161+ T conv (313 cells)
6 CD161+ T conv (103 cells)
7 44 cells
8 30 cells
tSNE1
tSNE2
c
CCR7
SELL
KLRB1
IL2RA
IL7R
FOXP3
tSNE_1
tSNE_2
High
Low
d
2636 cells
DUSP4
CCR7
FOXP1
PRDM1
NEDD9
KLRB1
TUBGCP2
NLRC5
IRF7
Z-score
e
scRNAseq
IL2RA
IL7R
FOXP3
KLRB1
SELL
CCR7
Expression (log2 UMI per 10,000)
Low
High
f
CyTOF
CD161+ Memory T conv
Memory T conv
Naive T conv
Naive T regs
Memory T regs
CD161+ T regs
Protein
Gene ID
CD25 IL2RA
CD127 IL7R
FOXP3 FOXP3
CD161 KLRB1
CD62L SELL
CCR7 CCR7
CD45RA PTPRC
CD45RO PTPRC
Signal intensity
Low
High
g
CD25
CD127
CD45RA
CD161
tSNE2
tSNE1
Max
Min
h
CD161+ memory T conv
Naive T regs
Memory T conv
Memory T regs
CD161+ T regs
Naive T conv

Supplementary Figure 1

CD161$^+$ T_{reg} cells are a discrete population of memory T_{reg} cells.

(**a**) Heat map showing signal intensity of selected markers for each node of the populations shown in Fig. 1c. (**b**–**e**) Clustering of populations of T_{conv} and T_{reg} cells by single-cell RNA-seq (scRNAseq) showing the tSNE plot of 2,636 cells from *n* = 3 independent donors separated into six major (clusters 0–6) and two minor (clusters 7 and 8) clusters (**b**), feature plots showing expression of three T_{reg} markers (*IL2RA* encoding CD25, *IL7R* encoding CD127 and *FOXP3* encoding FOXP3), *KLRB1* (encoding CD161) and two naive/memory markers (*SELL* encoding CD62L and *CCR7* encoding CCR7) (**c**), a heat map showing the top 20 discriminatory genes per cluster with representative genes of each cluster indicated (**d**) and population clustering (**e**) based on expression of the transcripts shown in **c**. Clusters in **b** are color-coded and labeled according to expression of the markers shown in **e**. (**f**) Clustering of T_{conv} and T_{reg} subpopulations using protein expression data sourced from CyTOF in Fig 1a incorporating the same markers as in **e** and also including CD45RA and CD45RO. Clustering of subpopulations in **f** is similar to that from scRNAseq (**e**). (**g**,**h**) viSNE plots (**g**) and 2D minimum spanning tree (**h**) of CD4$^+$ T cells clustered following staining with anti-CD4, anti-CD25, anti-CD127, anti-CD45RA and anti-CD161 for flow cytometry. Shown in **g** are heat maps for expression of the indicated markers, with an arrow indicating CD161 expression in T_{reg} cells. Node size in **h** represents cell number and color CD161 median intensity. Grouped together are naive (circled in orange), memory (circled in yellow) and CD161$^+$ (circled in purple) T_{reg} cells, as well as populations of naive (circled in black), memory (circled in black) and CD161$^+$ (circled in red) T_{conv} cells. The data in **g** and **h** are representative of *n* = 4 experiments. **P* < 0.01, ***P* < 0.001, ****P* < 0.0001 by one-way ANOVA.

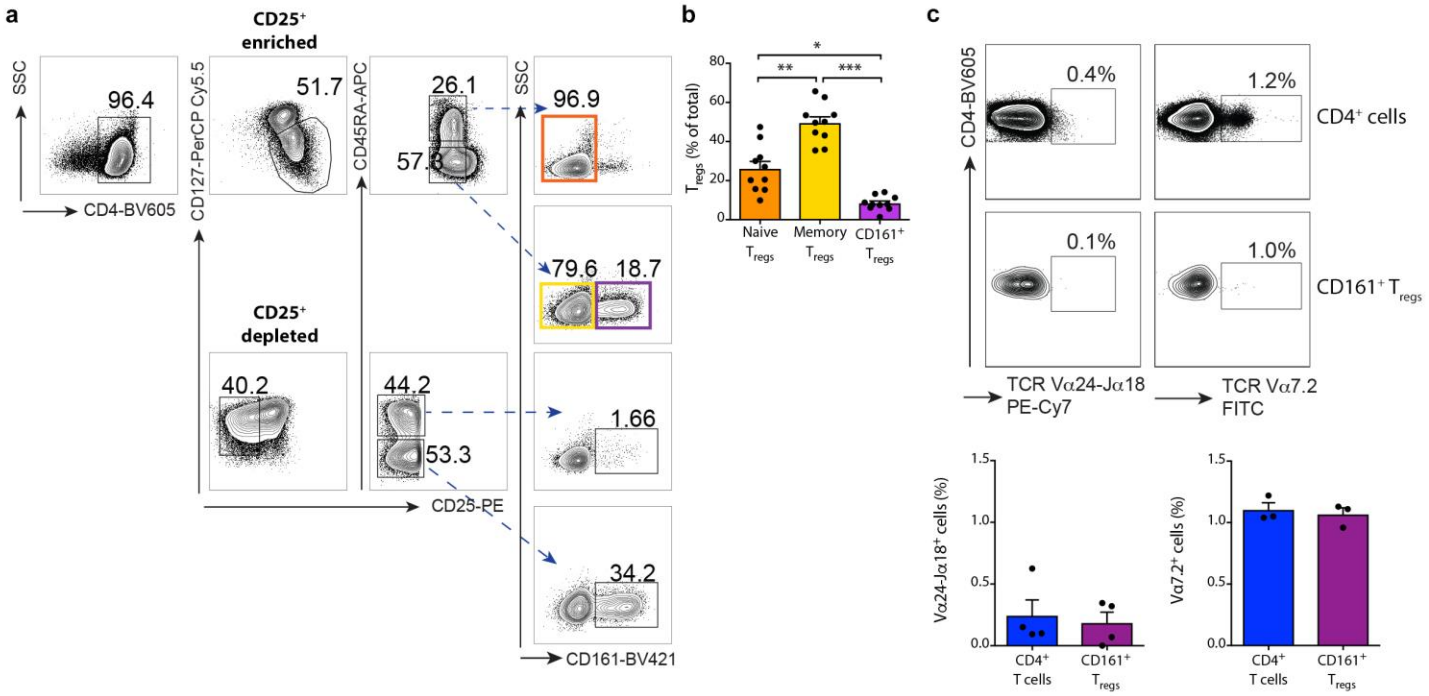
a
CD25+ enriched
SSC
96.4
CD4-BV605
CD127-PerCP Cy5.5
51.7
CD45RA-APC
26.1
57.8
SSC
96.9
79.6
18.7
CD25+ depleted
40.2
44.2
53.3
1.66
CD25-PE
34.2
CD161-BV421
b
Tregs (% of total)
Naive Tregs
Memory Tregs
CD161+ Tregs
c
CD4-BV605
0.4%
1.2%
CD4+ cells
0.1%
1.0%
CD161+ Tregs
TCR Vα24-Jα18 PE-Cy7
TCR Vα7.2 FITC
Vα24-Jα18+ cells (%)
Vα7.2+ cells (%)
CD4+ T cells
CD161+ Tregs

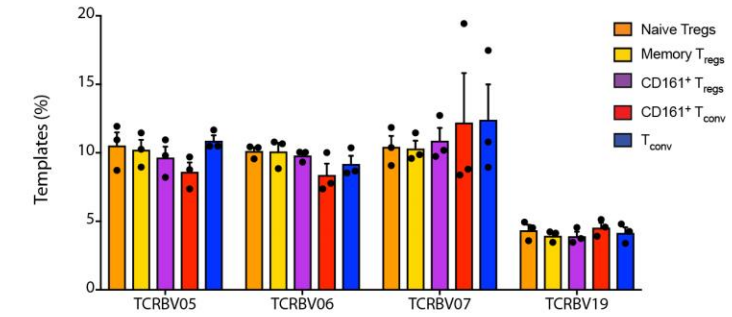
d
Templates (%)
Naive Tregs
Memory Tregs
CD161+ Tregs
CD161+ Tconv
Tconv
TCRBV05
TCRBV06
TCRBV07
TCRBV19

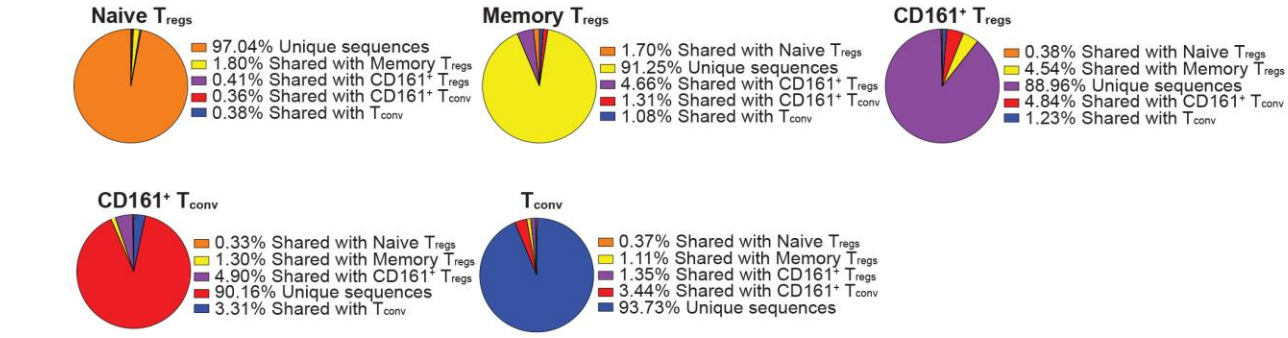
e
Naive Tregs
97.04% Unique sequences
1.80% Shared with Memory Tregs
0.41% Shared with CD161+ Tregs
0.36% Shared with CD161+ Tconv
0.38% Shared with Tconv
Memory Tregs
1.70% Shared with Naive Tregs
91.25% Unique sequences
4.66% Shared with CD161+ Tregs
1.31% Shared with CD161+ Tconv
1.08% Shared with Tconv
CD161+ Tregs
0.38% Shared with Naive Tregs
4.54% Shared with Memory Tregs
88.96% Unique sequences
4.84% Shared with CD161+ Tconv
1.23% Shared with Tconv
CD161+ Tconv
0.33% Shared with Naive Tregs
1.30% Shared with Memory Tregs
4.90% Shared with CD161+ Tregs
90.16% Unique sequences
3.31% Shared with Tconv
Tconv
0.37% Shared with Naive Tregs
1.11% Shared with Memory Tregs
1.35% Shared with CD161+ Tregs
3.44% Shared with CD161+ Tconv
93.73% Unique sequences

Supplementary Figure 2

CD161$^+$ T_{reg} cells are distinct from other CD161-expressing T cells.

(**a**) Representative example of the FACS sorting strategy for naive (orange), memory (yellow) and CD161$^+$ (purple) T_{reg} cells. (**b**) Proportions of each T_{reg} subpopulation in healthy human donor peripheral blood (cumulative data from n = 10 donors); bars show mean + s.e.m. (**c**) Representative (top) and cumulative (bottom) expression of TCR Vα24-Jα18 and Vα7.2 in total CD4$^+$ T cells and CD161$^+$ T_{reg} cells. Both cell types show minimal expression of these invariant TCR chains. Data are from n = 3 independent experiments. (**d**) Contribution of the three highest (BV05, BV06 and BV07) and one of the lowest (BV19) TCRBV families to the overall TCR repertoire in naive, memory and CD161$^+$ T_{reg} cells as well as CD161$^+$ and total T_{conv} cells. Data are from n = 3 independent experiments; bars show mean + s.e.m. (**e**) Average percentage of TCR sequences either unique or shared among naive, memory and CD161$^+$ T_{reg} cells, CD161$^+$ and total T_{conv} cells (cumulative data from n = 3 experiments). *P < 0.01, **P < 0.001, ***P < 0.0001 by one-way ANOVA.

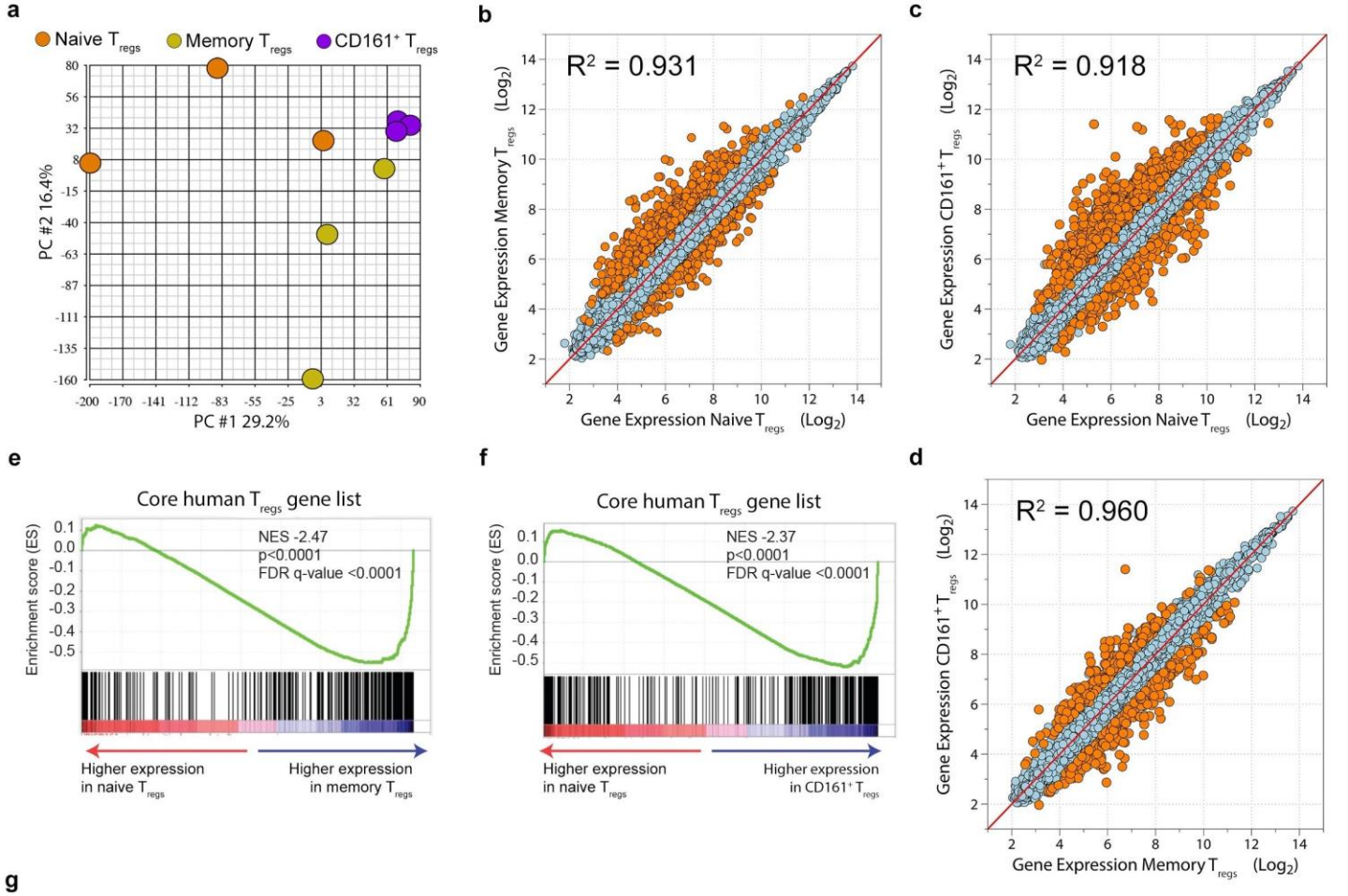
a
Naive T regs
Memory T regs
CD161+ T regs
PC #2 16.4%
PC #1 29.2%
b
R2 = 0.931
Gene Expression Memory T regs (Log2)
Gene Expression Naive T regs (Log2)
c
R2 = 0.918
Gene Expression CD161+ T regs (Log2)
Gene Expression Naive T regs (Log2)
e
Core human T regs gene list
NES -2.47
p<0.0001
FDR q-value <0.0001
Enrichment score (ES)
Higher expression in naive T regs
Higher expression in memory T regs
f
Core human T regs gene list
NES -2.37
p<0.0001
FDR q-value <0.0001
Enrichment score (ES)
Higher expression in naive T regs
Higher expression in CD161+ T regs
d
R2 = 0.960
Gene Expression CD161+ T regs (Log2)
Gene Expression Memory T regs (Log2)

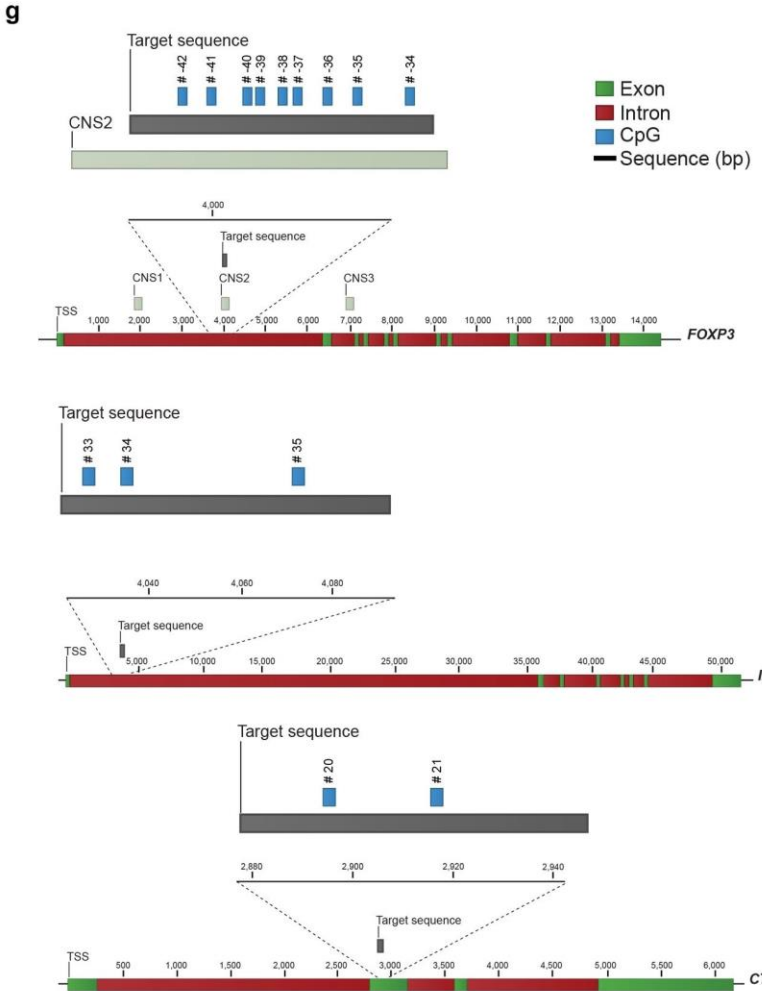
g
Target sequence
CNS2
Exon
Intron
CpG
Sequence (bp)
FOXP3
IL2RA
CTLA4
TSS

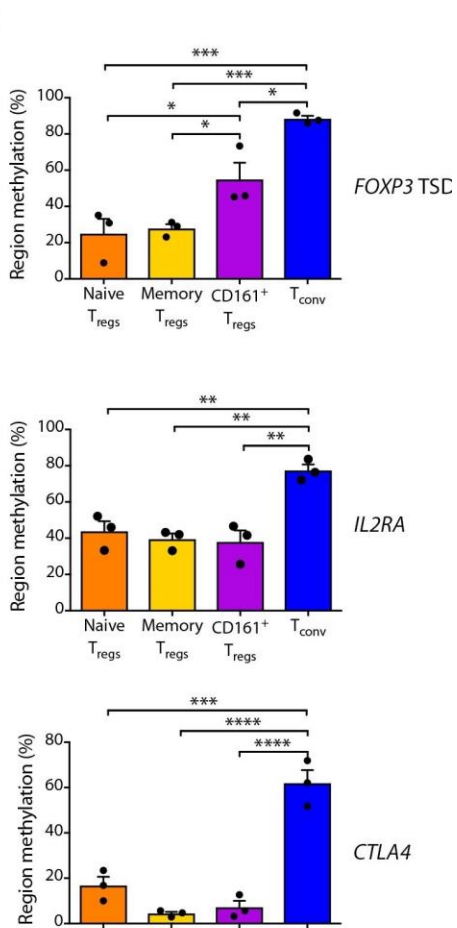
h
Region methylation (%)
Naive T regs
Memory T regs
CD161+ T regs
T conv
FOXP3 TSD
IL2RA
CTLA4

Supplementary Figure 3

Transcriptome and methylome of CD161$^+$ T_{reg} cells.

(**a**) Principal-component analysis (PCA) 2D mapping of variance in expression of transcripts in freshly isolated naive, memory and CD161$^+$ T_{reg} cells (*n* = 3). (**b**–**d**) Scatterplots showing correlation between mean gene expression of freshly isolated T_{reg} subpopulations (*n* = 3). (**e**,**f**) GSEA plots for core human T_{reg} signature genes comparing freshly isolated naive to memory T_{reg} cells (**e**) and to CD161$^+$ T_{regs} cells (**f**) (*n* = 3 per group). NES, normalized enrichment score; empirical *P* and multiple-test adjusted *q* values from GSEA are shown. (**g**) Schematic representation of *FOXP3*, *IL2RA* and *CTLA4* gene loci showing the target sequence and conserved CpGs assayed for methylation analysis in Fig. 2e. (**h**) Mean region methylation percentage of *FOXP3* TSDR, *IL2RA* and *CTLA4* loci from three male donors. Data are from *n* = 3 independent experiments; bars show mean + s.e.m. **P* < 0.05; ***P* < 0.01; ****P* < 0.001; *****P* < 0.0001 by one-way ANOVA.

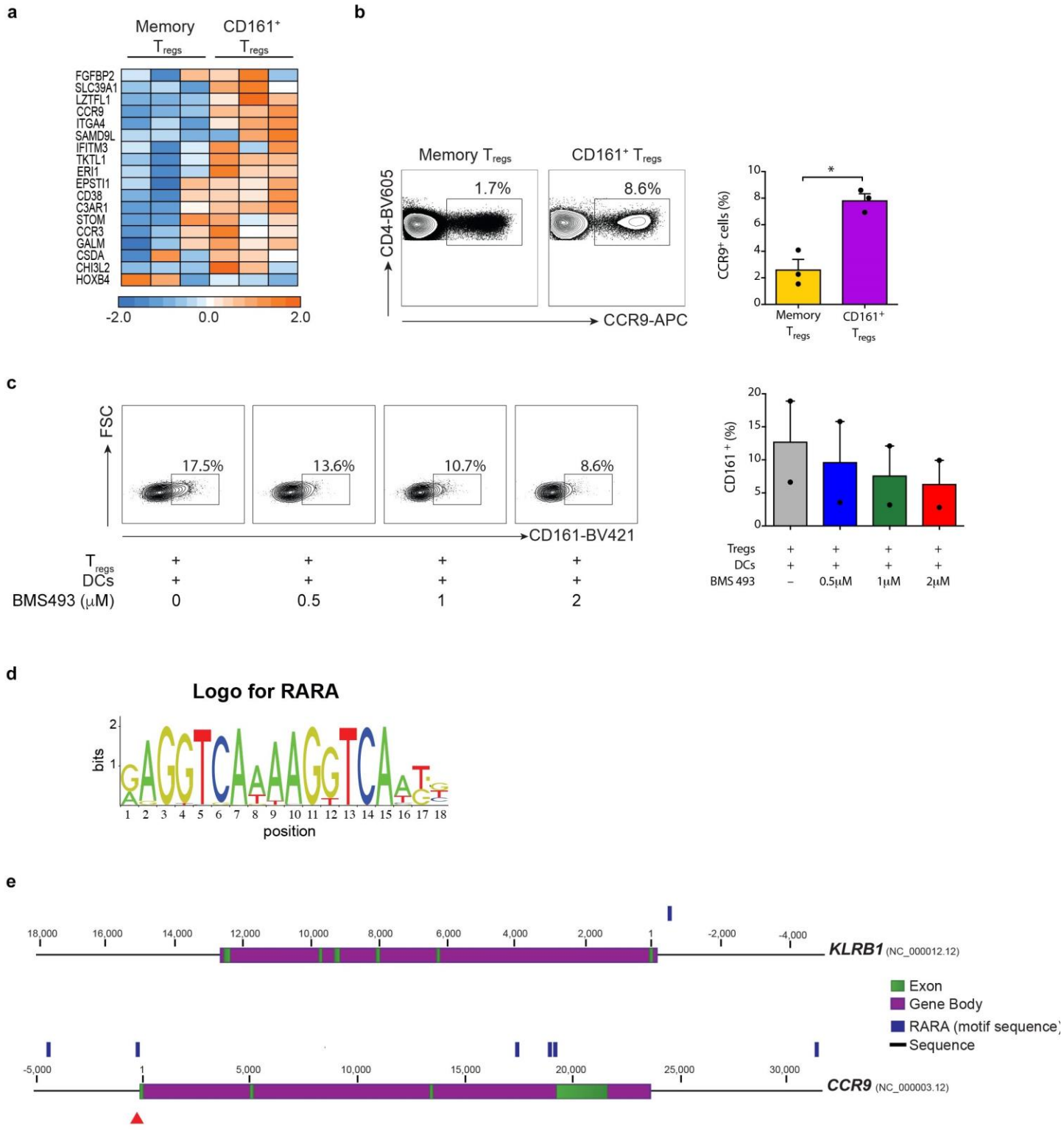

Supplementary Figure 4

Regulation of CD161 by retinoic acid.

(**a**) Heat map of leading edge (core enriched) genes from GSEA for ATRA-regulated genes comparing freshly isolated memory to CD161^{+} T_{reg} cells (Fig. 3a). Data are from *n* = 3 independent experiments. (**b**) CCR9

surface protein expression on memory and CD161^{+} T_{reg} cells; shown are representative flow cytometry plots (left) and cumulative data from *n* = 3 independent experiments (right). (**c**) CD161 expression on T_{reg} cells co-cultured for 5 d with DCs with and without BMS493 at increasing concentrations. Shown are representative plots (left) and cumulative data (right) from *n* = 3 independent experiments. (**d**,**e**) Sequence logo for RARA DNA motif (**d**) and schematic representation of the *KLRB1* and *CCR9* gene loci (±5 kb) showing the predicted binding sites of RARA (**e**); the red arrowhead indicates the binding site for *CCR9* selected for analysis in ChIP–qPCR. Bars show mean + s.e.m. throughout the figure. *$P < 0.05$ by paired *t*-test.

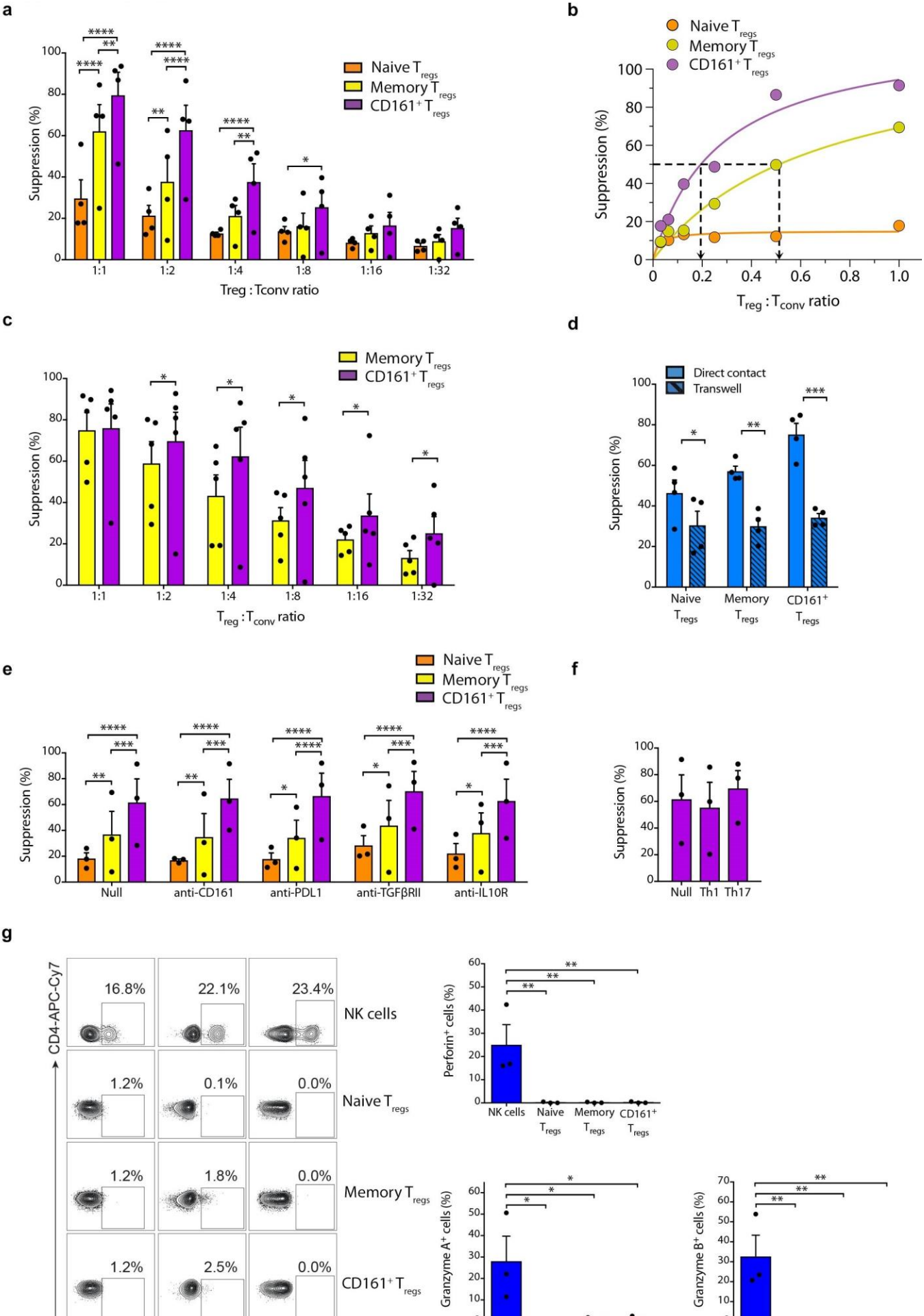
a
Naive T regs
Memory T regs
CD161+ T regs
Suppression (%)
Treg : Tconv ratio
1:1
1:2
1:4
1:8
1:16
1:32
b
Naive T regs
Memory T regs
CD161+ T regs
Suppression (%)
Treg : Tconv ratio
c
Memory T regs
CD161+ T regs
Suppression (%)
Treg : Tconv ratio
d
Direct contact
Transwell
Suppression (%)
Naive Tregs
Memory Tregs
CD161+ Tregs
e
Naive T regs
Memory T regs
CD161+ T regs
Suppression (%)
Null
anti-CD161
anti-PDL1
anti-TGFβRII
anti-IL10R
f
Suppression (%)
Null
Th1
Th17
g
CD4-APC-Cy7
16.8%
22.1%
23.4%
NK cells
1.2%
0.1%
0.0%
Naive Tregs
1.2%
1.8%
0.0%
Memory Tregs
1.2%
2.5%
0.0%
CD161+ Tregs
Perforin+ cells (%)
NK cells
Naive Tregs
Memory Tregs
CD161+ Tregs
Granzyme A+ cells (%)
Granzyme B+ cells (%)

Supplementary Figure 5

CD161$^+$ T_{reg} cells are highly regulatory.

(**a**,**b**) Cumulative mean percentage suppressive function of freshly isolated naive, memory and CD161$^+$ T_{reg} cells from Fig. 4a (*n* = 4 experiments) (**a**) and representative IC_{50} value calculation (**b**; dashed arrows show the IC_{50} for CD161$^+$ and memory T_{reg} cells). (**c**) Cumulative mean percentage suppressive function of memory and CD161$^+$ T_{reg} cells after in vitro expansion for 2 weeks (*n* = 4 experiments). (**d**) Suppression of T_{conv} cell proliferation when in direct contact with T_{reg} cells or when separated by a Transwell at a T_{reg}:T_{conv} ratio of 1:1 (cumulative data from *n* = 4 independent experiments). (**e**) Suppressive function of T_{reg} cells under neutral (null) conditions or in the presence of blocking antibodies directed against CD161, PDL1, TGFβRII or IL10R, all at a T_{reg}:T_{conv} ratio of 1:2 (cumulative data from *n* = 3 independent experiments). (**f**) Suppressive function of CD161$^+$ T_{reg} cells under neutral (null) conditions or in the presence of T_H1 and T_H17 skewing conditions, all at a T_{reg}:T_{conv} ratio of 1:2 (cumulative data from *n* = 3 independent experiments). (**g**) Expression of perforin, granzyme A and B in subpopulations of T_{reg} cells, with NK cells as a positive control; shown are representative flow cytometry plots for each marker (left) and cumulative data from *n* = 3 independent experiments (right). Bar charts show mean + s.e.m. throughout the figure. **P* < 0.05, ***P* < 0.01, ****P* < 0.001, *****P* < 0.0001 by two-way ANOVA (**a**–**e**) and one-way ANOVA (**g**).

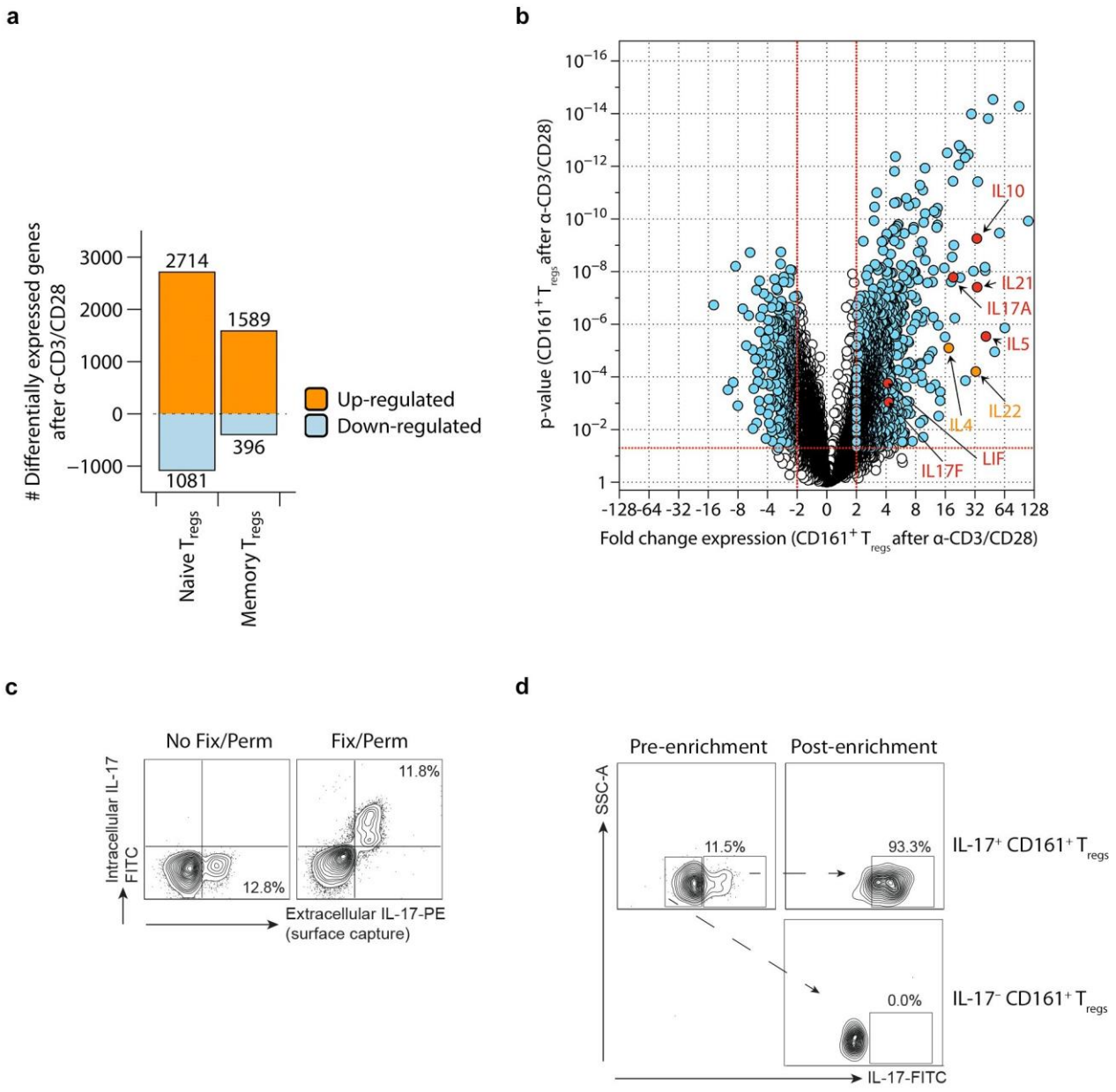

Supplementary Figure 6

CD161$^+$ T_{reg} cells produce multiple cytokines upon activation.

(**a**) Differentially expressed genes (at least twofold change at $P < 0.05$) following 4 h of stimulation of memory and naive T_{reg} cells with anti-CD3/CD28. (**b**) Volcano plot showing significant genes differentially expressed in CD161$^+$ T_{reg} cells after 4 h of activation with anti-CD3/CD28. Differentially expressed genes are shown in blue; red indicates significantly upregulated cytokine genes that are differentially expressed compared to memory T_{reg} cells (see Fig. 5c); orange indicates other cytokine genes of interest upregulated in activated CD161$^+$ T_{reg} cells. The data in **a** are **b** are from three independent experiments. (**c**,**d**) Cell sorting of IL-17$^+$ and IL-17$^-$ CD161$^+$ T_{reg} cells by surface IL-17 capture. Shown are representative flow cytometry plots with double staining for intracellular and extracellular (captured on the surface) IL-17 with (right) and without (left) fixation and permeabilization (**c**) and the sorting strategy using IL-17 surface capture and post-sorting purity for the IL-17$^+$ and IL-17$^-$ fractions of CD161$^+$ T_{reg} cells (**d**). Shown in **c** and **d** are representative examples from $n = 3$ and $n = 4$ independent experiments, respectively.

a

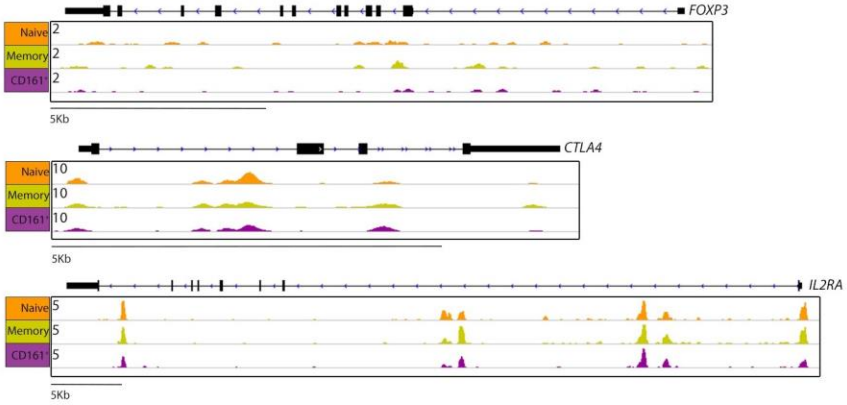

b

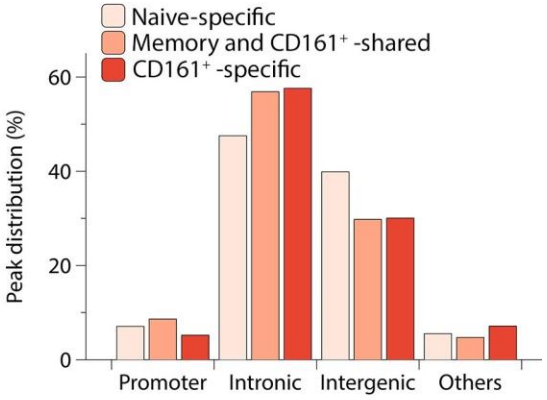

c

Transcription Factor	Motif	P-value: Naïve specific	P-value: Memory and CD161$^+$ shared	P-value: CD161$^+$ specific
BACH1		1	1 x 10^{-23}	1 x 10^{-12}
BACH2		1	1 x 10^{-44}	1 x 10^{-23}
NF-E2		1	1 x 10^{-26}	1 x 10^{-8}
NRF2		1	1 x 10^{-19}	1 x 10^{-9}
JUN-AP1		1	1 x 10^{-71}	1 x 10^{-49}
FOSL2		1	1 x 10^{-75}	1 x 10^{-50}
FRA1		1	1 x 10^{-61}	1 x 10^{-53}
BATF		1	1 x 10^{-59}	1 x 10^{-50}
AP-1		1	1 x 10^{-58}	1 x 10^{-51}
ATF3		1	1 x 10^{-59}	1 x 10^{-56}
MAFK		1	1 x 10^{-15}	1 x 10^{-6}
RORC		1	1 x 10^{-14}	1 x 10^{-30}
ETS:RUNX		1 x 10^{-5}	1 x 10^{-6}	1x 10^{-14}
ETS1-distal		1 x 10^{-14}	1 x 10^{-13}	1 x 10^{-12}
ELK1		1 x10^{-7}	1 x 10^{-17}	1 x 10^{-12}
ELK4		1 x 10^{-4}	1 x 10^{-15}	1 x 10^{-11}
ELF1		1x 10^{-5}	1 x 10^{-13}	1 x 10^{-6}
RUNX		1x 10^{-5}	1 x 10^{-32}	1 x 10^{-21}
TCF3		1 x 10^{-16}	1 x 10^{-2}	1
TCF4		1 x 10^{-14}	1 x 10^{-1}	1

d

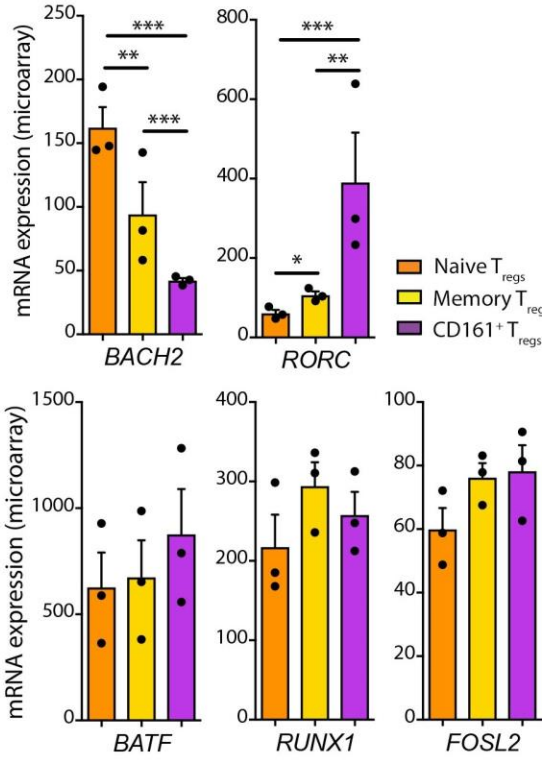

e

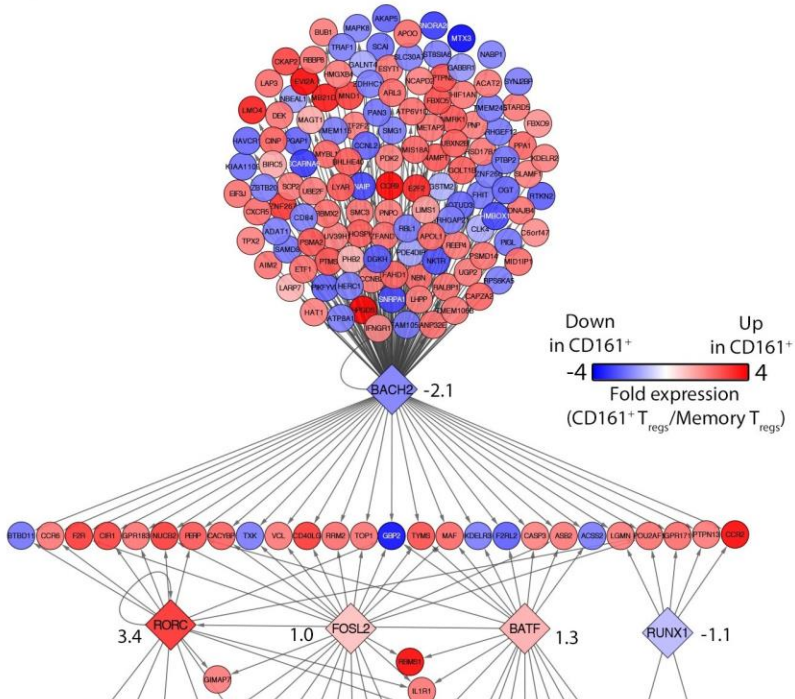

Supplementary Figure 7

Global analysis of T_{reg} regulomes.

(**a**) Open chromatin regions (OCRs) at prototypical T_{reg} gene loci from Fig. 6a. (**b**) Genomic distribution of ATAC peaks (promoter, intragenic or intergenic regions) in the three groups shown in Fig. 6a. (**c**) *P* values (cumulative hypergeometric test *P* values calculated by Homer) for transcription factor (TF) motifs shown in each cluster in Fig. 6c. Data in **a**–**c** are from *n* = 3 experiments. (**d**) Expression of key TFs participating in gene regulation in $CD161^+$ T_{reg} cells. Shown is the normalized signal intensity (mean + s.e.m.) from *n* = 3 microarrays for each T_{reg} population. (**e**) Integrated TF network showing the contribution of each TF to DEGs and overlap between them (fold difference in expression of each TF is also indicated next to the TF). **P* < 0.05, ***P* < 0.01, ****P* < 0.001 (Partek analysis of microarrays).

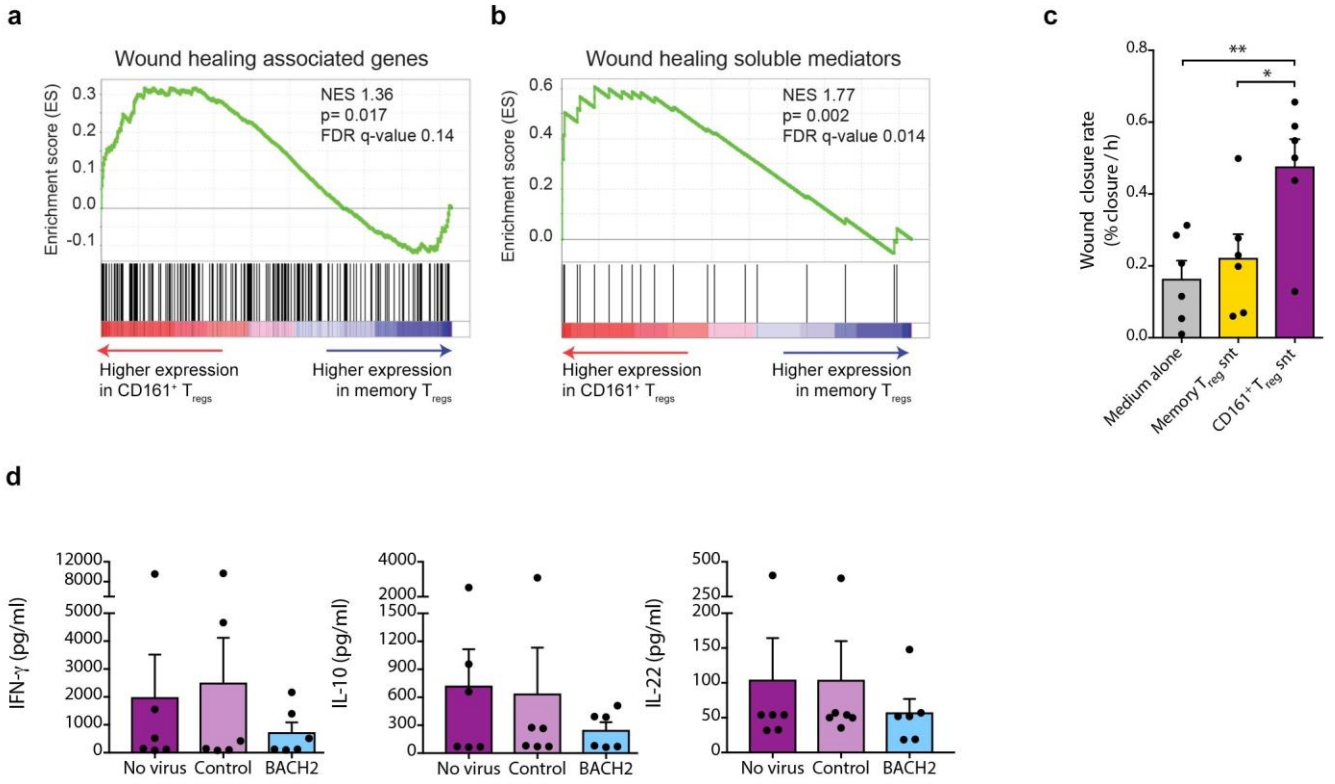

Supplementary Figure 8

CD161$^+$ T_{reg} cells accelerate wound healing.

(**a**,**b**) GSEA plots for wound healing–associated genes (**a**) and wound healing–associated soluble mediators (**b**) comparing activated CD161$^+$ to memory T_{reg} cells. Data are from *n* = 3 independent experiments. NES, normalized enrichment score; empirical *P* and multiple-test-adjusted *q* values from GSEA are indicated. (**c**) Wound closure rate of Caco-2 cells cultured in the presence of either medium alone or medium supplemented with culture supernatants (snt) from activated memory or CD161$^+$ T_{reg} cells. Shown are cumulative data from *n* = 6 independent experiments. (**d**) Concentration (pg/ml) of stated cytokines in supernatants of CD161$^+$ T_{reg} cells transduced, or not, with control lentivirus or lentivirus encoding BACH2 (cumulative data from *n* = 6 experiments)**.** Bar charts show mean + s.e.m.; **P* < 0.05, ***P* < 0.01 by one-way ANOVA.